

X-Ray Determination of the Molecular Tilt and Layer Fluctuation Profiles of Freely Suspended Liquid-Crystal Films

Douglas J. Tweet,⁽¹⁾ Robert Hołyst,^{(1),(2)} Brian D. Swanson,⁽¹⁾ Hans Stragier,⁽¹⁾ and Larry B. Sorensen⁽¹⁾

⁽¹⁾*Department of Physics FM-15, University of Washington, Seattle, Washington 98195*

⁽²⁾*Institute of Physical Chemistry of the Polish Academy of Sciences, Department III, Kasprzaka 44/52, 01224 Warsaw, Poland*

(Received 8 June 1990)

X-ray diffraction has been used to study the interlayer structure of fluid freely suspended liquid-crystal films versus film thickness. The observed scattering is described extremely well by a simple interlayer density model based on predicted layer fluctuation σ_i and tilt angle ϕ_i profiles. The diffraction data determine the individual σ_i 's to about $\pm 0.1 \text{ \AA}$, and the layer fluctuation profiles calculated for the hydrodynamic fluctuations agree to this precision. The tilt profiles calculated using a simple elastic theory are also in excellent agreement with the data.

PACS numbers: 61.30.Eb, 61.10.-i, 68.15.+e, 68.90.+g

Liquid crystals allow us to study systems with symmetries and order intermediate between isotropic liquids and fully ordered crystals.¹ Freely suspended liquid-crystal (FSLC) films have been used to study the two-dimensional to three-dimensional crossover of the intralayer order in these systems.^{1,2} In thin FSLC films, the influence of the surface is very important: There are surface-induced phases in the interior of the film that can be several hundred layers thick,³ there are surface-induced tilt changes,⁴ and there are monolayer⁵ and multilayer⁶ surface-induced freezing transitions. In this Letter, we describe the use of x-ray scattering techniques to directly determine the *interlayer* structure in thin FSLC films versus film thickness. We show that the finite size and the surface tension quench the bulk smectic-layer fluctuations, and that the measured fluctuations are in quantitative agreement ($\pm 0.1 \text{ \AA}$) with the fluctuation amplitudes predicted in the companion Letter.⁷ We also show that the surface-frozen monolayers induce a tilt profile into the interior layers, and present a simple phenomenological theory for the tilt profile which agrees with the measured profile.

The x-ray scattering measurements were made using a triple-axis spectrometer. The monochromator and analyzer crystals were flat ZYX pyrolytic graphite. To increase the effective instrument resolution and to prevent the incident beam from illuminating the film holder, the monochromator and analyzer in-plane slits were set narrower than the graphite acceptance. The resulting longitudinal resolution, $\Delta Q_z = 0.009 \text{ \AA}^{-1}$ FWHM, was comparable to the corresponding finite-size FWHM for a 21-layer film. The resolution perpendicular to the scattering plane, $\Delta Q_\perp \approx 0.04 \text{ \AA}^{-1}$ FWHM, was determined by the out-of-plane slit settings; this resolution was wide enough to collect all of the out-of-plane scattering. The x-ray source was a rotating anode generator operated at 5 kW with a small focus gun (0.3 mm \times 3 mm). Copper $K\alpha_1$ radiation, $\lambda = 1.5406 \text{ \AA}$, was used; the $K\alpha_2$ line was blocked by slits placed near the parafocusing point of the monochromator. To determine

the interlayer density profile, the x-ray scattering intensities were measured with the momentum transfer Q_z perpendicular to the smectic layers. To facilitate the measurements at small Q_z , we used large freely suspended films (8 cm \times 1.25 cm) supported by a thin (125 μm) stainless-steel aperture. These large films had a layer mosaic spread of about 0.2° FWHM. To obtain reliable intensity measurements, all the scans were mosaic averaged.

The liquid crystal, 4-(*n*-heptyl)oxybenzylidene-4-(*n*-heptyl)aniline (7O.7), was chosen for this study because the thickness dependence of its phase diagram has been thoroughly studied.³ Experiments were performed at 72.5°C where the film is in a phase, denoted smectic-*I/C*, which consists of monolayer 2D hexatic, smectic-*I* surface layers on a 2D fluid, smectic-*C* interior.⁵ This allowed measurements of the effect of the surface-induced hexatic phase on the fluid smectic-*C* interior.

All of the measured scattering data can be described by the simple model shown schematically in Fig. 1. The

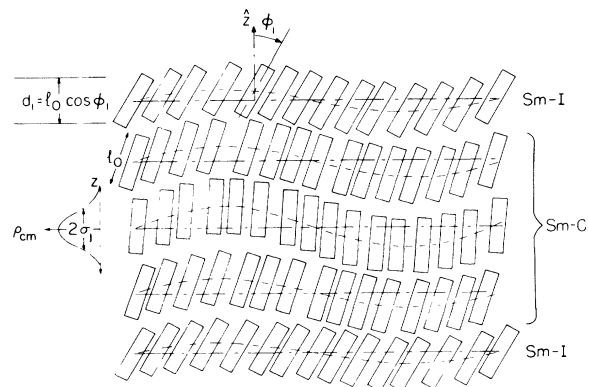


FIG. 1. Schematic illustration of the fluctuations in a 5-layer smectic-*I/C* film (see text). The two surface layers are smectic *I* and the three interior layers are smectic *C*. Note the variation in the tilt angle and in the magnitude of the layer fluctuations with z .

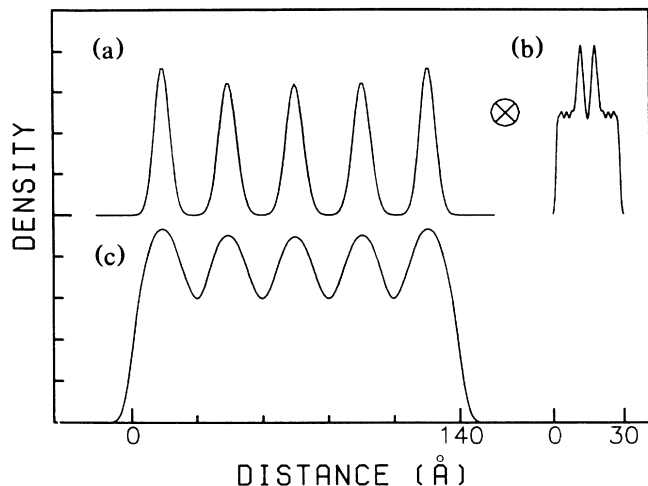


FIG. 2. Interlayer density model for a 5-layer smectic-I/C film. (a) Normalized Gaussian center-of-mass distributions. The Gaussians are narrower near the surface. (b) Projected electron density of a 70.7 molecule. (c) Total electron density of the film, calculated by convolving the tilt-dependent molecular density for each layer with its Gaussian and summing over the layers.

70.7 molecules, represented by rectangles, form fluctuating smectic layers. The static equilibrium layer positions are indicated by the parallel lines perpendicular to the z axis. The thermally excited, long-wavelength hydrodynamic fluctuations of the layers are illustrated schematically by the dashed lines indicating the instantaneous molecular center-of-mass locations. The molecular center-of-mass distribution along z of the j th layer is parametrized by a normalized Gaussian distribution with width σ_j . Notice that this width is smallest at the surface, because of the surface tension, and that the molecular tilt angle for the i th layer, ϕ_i , is largest for the surface layers and decreases further into the film. Assuming rigid molecules with length l_0 ,⁸ the tilt couples to the layer thickness d_i via $d_i = l_0 \cos \phi_i$.

For the model shown in Fig. 1, $\rho(z)$, the projection of the electron density onto the z axis, is given by

$$\rho(z) = \sum_i (2\pi\sigma_i^2)^{-1/2} \exp\left[-\frac{(z-z_i)^2}{2\sigma_i^2}\right] \otimes M_i(z), \quad (1)$$

where \otimes denotes convolution. The center-of-mass distribution of the i th layer is given by the normalized Gaussian centered at z_i with width σ_i ; the Gaussian form is a direct consequence of the Hamiltonian used to calculate

$$F = \int_{-D/2}^{+D/2} \left\{ c_1 [\phi(z) - \phi_B]^2 + c_2 [\phi'(z)]^2 + c_3 [\phi(z) - \phi_S]^2 \left[\delta\left(z - \frac{D}{2}\right) + \delta\left(z + \frac{D}{2}\right) \right] \right\} dz, \quad (2)$$

where $\phi'(z) \equiv d\phi(z)/dz$ and D is the film thickness. In this equation, c_1 and c_3 are the elastic constants associated with distortions of $\phi(z)$ from the preferred tilt angle in the interior, ϕ_B , and at the surface, ϕ_S , respectively, while c_2 is the

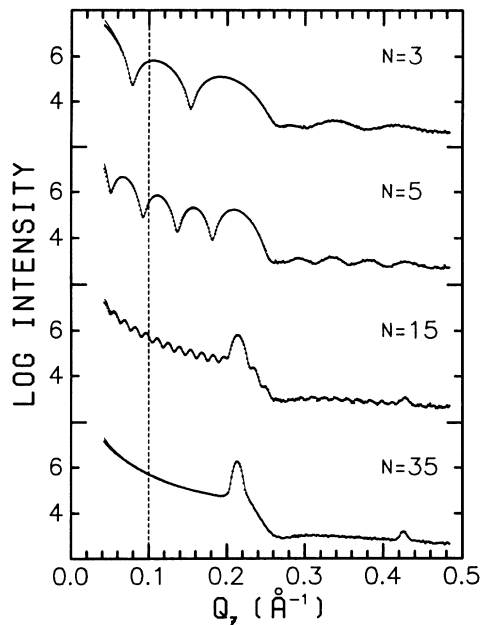


FIG. 3. Comparison of the measured scattering with the tilt and fluctuation profile fits for 3-, 5-, 15-, and 35-layer smectic-I/C films. Note the excellent agreement between the data (dots) and fits (solid line). The subsidiary maxima characteristic of N -layer systems are clearly visible. The data to the left of the dotted line, $Q_z \leq 0.1 \text{ \AA}^{-1}$, were not used in the fits, because the projected x-ray beam was larger than the sample and illuminated the film aperture.

the fluctuations.⁹ The electron density for the i th layer is given by the center-of-mass Gaussian convolved with the molecular density $M_i(z)$. Both $M_i(z)$ and z_i depend on the tilt of the molecules, ϕ_i , with respect to z ; $M_i(z)$ was calculated from the known atomic structure of the molecule and symmetrized to reflect the equal probabilities of molecules oriented along and opposite to the director. The contributions from each layer were added together to produce $\rho(z)$, as illustrated in Fig. 2. The scattering intensities were calculated by Fourier transforming $\rho(z)$ and including the instrument resolution and scattering geometry.^{9,10} The agreement between the data and the calculated intensities over more than 4 orders of magnitude is shown in Fig. 3.

The fits shown in Fig. 3 use theoretically predicted tilt and fluctuation profiles, ϕ_i and σ_i . As described below, both of these profiles have three thickness-independent parameters, so all the data were fitted by adjusting six parameters.

The tilt profile was calculated using the simple phenomenological free energy,⁹

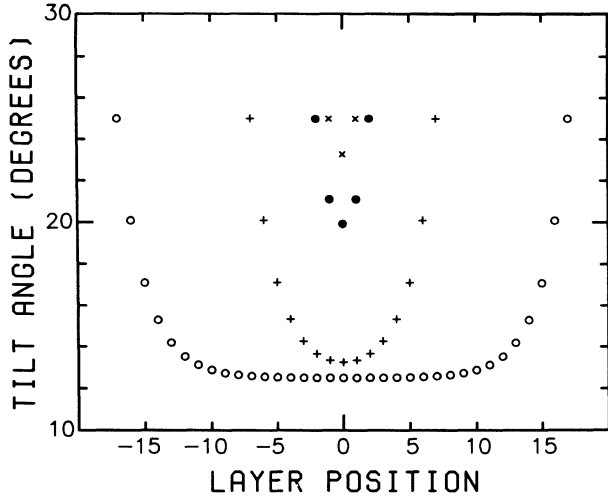


FIG. 4. Molecular tilt angle profiles ϕ_i for 3- (\times), 5- (\bullet), 15- ($+$), and 35- (\circ) layer smectic-I/C films calculated using Eq. (3).

elastic constant associated with the spatial variations of $\phi(z)$. Minimizing F with respect to $\phi(z)$ and solving the resulting equations, we find

$$\phi(z) = \frac{(\phi_S - \phi_B) \cosh(z/\xi)}{\cosh(D/2\xi)} + \phi_B, \quad (3)$$

where $\xi = \sqrt{c_2/c_1}$ is the tilt decay length. Equation (3) assumes that the hexatic surface layers are much stiffer than the interior fluid layers, $c_3 \gg \sqrt{c_2 c_1}$.

The predicted tilt profile $\phi(z)$ given by Eq. (3) was used in the fits. The free parameters in these fits were ϕ_S , ϕ_B , and ξ . All the data were fitted by a single set of parameters: $\phi_S = 25^\circ \pm 0.5^\circ$, $\phi_B = 12.5^\circ \pm 1^\circ$, and $\xi = (1.9 \pm 0.1)d$, where d is the average layer spacing. The tilt profiles ϕ_i determined by the fits are shown in Fig. 4. Since the surface smectic-I layers have a larger preferred tilt than the smectic-C interior layers, the smectic-C layers near each surface are more tilted than the interior layers. For thick films, the tilt profile decays from ϕ_S at the surface to ϕ_B in the center. These profiles also show that thin films are more tilted than thick films.⁴

As explained in detail in the companion Letter,⁷ the layer fluctuations are dominated by hydrodynamic, long-wavelength fluctuations, and can be calculated for finite films using a Landau-de Gennes smectic-A free energy modified to include the surface tension. The fits used layer fluctuation profiles σ_i calculated using the formalism developed in Ref. 7. The free parameters in these fits were the smectic elastic constants, B and K , and the surface tension γ . The values obtained from the fits show that γ and $\beta \equiv \sqrt{BK}$ are well determined (i.e., the product of B and K is well determined, but the individual values are not). The best-fit values were $\gamma = 25 \pm 2$ dyn/cm, independent of the number of layers, N , and

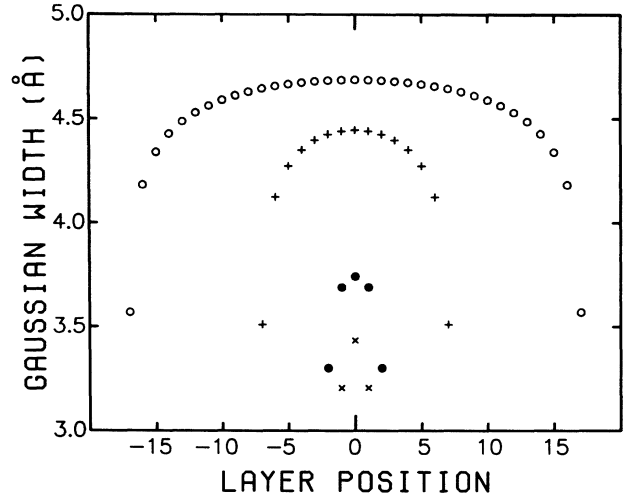


FIG. 5. Layer fluctuation profiles σ_i for 3- (\times), 5- (\bullet), 15- ($+$), and 35- (\circ) layer smectic-I/C films calculated using the theory in Ref. 7.

$\beta(N)$ given by $N\beta(N) = 2\beta_I + (N-2)\beta_C$, with the surface value $\beta_I = 11.7 \pm 0.7$ dyn/cm and the bulk value $\beta_C = 5.2 \pm 0.3$ dyn/cm. The fluctuation profiles σ_i used in the fits are shown in Fig. 5. The qualitative features of these fluctuation profiles are as follows: The surface fluctuations are suppressed by the surface tension; the fluctuations increase rapidly over the first few layers away from each free surface; and the fluctuation profiles are parabolic near the center of the films.

In conclusion, we have shown that (1) very detailed interlayer structural information can be obtained from x-ray scattering studies of thin liquid-crystal films. (2) The observed scattering is described extremely well by a simple interlayer density model with Gaussian disorder of the layers. (3) Smectic-I/C 70.7 films have distinct tilt and layer fluctuation profiles. The tilt profile is induced by the surface-frozen smectic-I phase and is in quantitative agreement with a simple elastic theory. The layer fluctuation profile agrees to ± 0.1 Å with a direct calculation⁷ of the hydrodynamic layer fluctuations. In addition, the surface layers are more tilted and more ordered than the interior layers, and the interiors of thin films are more tilted and more ordered than the interiors of thicker films.

We gratefully acknowledge support of this research by the M. J. Murdock Charitable Trust, the University of Washington Graduate School Research Fund, and the National Science Foundation under Grants No. DMR-8612286 and No. DMR-8916052.

¹P. S. Pershan, *Structure of Liquid Crystal Phases* (World Scientific, Singapore, 1988).

²For very recent work, see, J. D. Brock, R. J. Birgeneau, J. D. Litster, and A. Aharony, *Cont. Phys.* **30**, 321 (1989), and

references therein; D. Y. Noh, J. D. Brock, J. O. Fossum, J. P. Hill, J. Nuttall, J. D. Litster, and R. J. Birgeneau (to be published).

³E. B. Sirota, P. S. Pershan, L. B. Sorensen, and J. Collett, *Phys. Rev. A* **36**, 2890 (1987); *Phys. Rev. Lett.* **55**, 2039 (1985); J. Collett, P. S. Pershan, E. B. Sirota, and L. B. Sorensen, *Phys. Rev. Lett.* **52**, 356 (1984).

⁴S. M. Amador and P. S. Pershan, *Phys. Rev. A* **41**, 4326 (1990); S. Heinekamp, R. A. Pelcovits, E. Fontes, E. Y. Chen, R. Pindak, and R. B. Meyer, *Phys. Rev. Lett.* **52**, 1017 (1984); C. Rosenblatt, R. Pindak, N. A. Clark, and R. B. Meyer, *Phys. Rev. Lett.* **42**, 1220 (1979).

⁵S. Amador, P. S. Pershan, H. Stragier, B. D. Swanson, D. J. Tweet, L. B. Sorensen, E. B. Sirota, G. E. Ice, and A. Habenschuss, *Phys. Rev. A* **39**, 2703 (1989); E. B. Sirota, P. S. Pershan, S. Amador, and L. B. Sorensen, *Phys. Rev. A* **35**,

2283 (1987).

⁶B. D. Swanson, H. Stragier, D. J. Tweet, and L. B. Sorensen, *Phys. Rev. Lett.* **62**, 909 (1989).

⁷R. Hołyst, D. J. Tweet, and L. B. Sorensen, preceding Letter, *Phys. Rev. Lett.* **65**, 2153 (1990).

⁸C. R. Safinya, M. Kaplan, J. Als-Nielsen, R. J. Birgeneau, D. Davidov, J. D. Litster, D. L. Johnson, and M. E. Neubert, *Phys. Rev. B* **21**, 4149 (1980).

⁹D. J. Tweet, R. Hołyst, B. D. Swanson, H. Stragier, and L. B. Sorensen (to be published).

¹⁰See, for example, B. E. Warren, *X-Ray Diffraction* (Addison-Wesley, New York, 1969). To convert from $\rho(z)$ to $I(Q_z)$ we multiplied the complex modulus squared of the Fourier transform of $\rho(z)$ by $(1 + \cos^2 2\theta)/2 \sin\theta \sin 2\theta$ and then convolved with the instrument resolution. In this expression 2θ is the scattering angle.